Secondary Structure and Position of the Cell-Penetrating Peptide Transportan in SDS Micelles As Determined by NMR†

Mattias Lindberg,‡ Jüri Jarvet,‡ Ülo Langel,§ and Astrid Gräslund*,‡

Department of Biochemistry and Biophysics and Department of Neurochemistry and Neurotoxicology, The Arrhenius Laboratories, Stockholm University, S-106 91 Stockholm, Sweden

Received April 20, 2000; Revised Manuscript Received October 6, 2000

ABSTRACT: Transportan is a 27-residue peptide (GWTLN SAGYL LGKIN LKALA ALAKK IL-amide) which has the ability to penetrate into living cells carrying a hydrophilic load. Transportan is a chimeric peptide constructed from the 12 N-terminal residues of galanin in the N-terminus with the 14-residue sequence of mastoparan in the C-terminus and a connecting lysine. Circular dichroism studies of transportan and mastoparan show that both peptides have close to random coil secondary structure in water. Sodium dodecyl sulfate (SDS) micelles induce 60% helix in transportan and 75% helix in mastoparan. The 600 MHz ^{1}H NMR studies of secondary structure in SDS micelles confirm the helix in mastoparan and show that in transportan the helix is localized to the mastoparan part. The less structured N-terminus of transportan has a secondary structure similar to that of the same sequence in galanin [Öhman, A., et al. (1998) *Biochemistry 37*, 9169−9178]. The position of mastoparan and transportan relative to the SDS micelle surface was studied by adding spin-labeled 5-doxyl- or 12-doxyl-stearic acid or Mn^{2+} to the peptide/micelle system. The combined results show that the peptides are for the most part buried in the SDS micelles. Only the C-terminal parts of both peptides and the central segment connecting the two parts of transportan are clearly surface exposed. For mastoparan, the secondary chemical shifts of the amide protons were found to vary periodically and display a pattern almost identical to those reported for mastoparan in phospholipid bicelles [Vold, R., et al. (1997) *J. Biomol. NMR 9*, 329−335], indicating similar structures and interactions in the two membrane-mimicking environments.

The problem of making large hydrophilic compounds pass through biological membranes and enter living cells has for a long time remained difficult. It was discovered relatively recently that a short peptide with a sequence derived from the DNA binding domain (homeodomain) of the Antennapedia transcription factor in *Drosophila* was translocated across the plasma membrane and into the nucleus of living cells (*1*) and that it could also carry large cargo molecules with it (*2*). This led to a wider search for other translocating peptide sequences, and a few other classes have been found, e.g., so-called tat-derived peptides (*3*), peptides based on signal sequences (*4*, *5*), or purely synthetic or chimeric peptide sequences (*6*). A recent review summarizes some present knowledge about these membrane translocating peptides (*7*). Transportan is a 27-amino acid peptide with a sequence based on the N-terminal fragment of residues 1−12 of the neuropeptide galanin fused with the sequence of the wasp venom mastoparan (14 amino acids) via a linking lysine residue. Its sequence is GWTLN^5 SAGYL^{10} LGKIN^{15} LKALA^{20} ALAKK^{25} IL-amide). Like the other cell-penetrating peptides, it has a number of positively charged residues and in addition some hydrophobic ones.

Various biological effects of transportan and its predecessor, galparan, have been characterized before. It has been demonstrated that these peptides stimulate the release of acetylcholine in the frontal cortex of rats (*8*), while galanin is known to inhibit evoked acetylcholine release in the hippocampus. Similar results were obtained when the influence of galparan on glucose-induced insulin release was measured. Galanin is known to inhibit the insulin release, whereas galparan on the contrary strongly stimulates the release in rat pancreatic islets (*9*). Mastoparan has a small insulin-releasing effect.

Basal GTPase activity in Bowes cell membranes is reduced to 20% by 100 μM biotinyl-transportan with an EC_{50} of 21 μM. The strong inhibitory action of biotinyl-transportan on GTPases is probably caused by direct interaction of the peptide with the enzyme or by influencing the properties of the biomembrane surrounding it.

Various regulators of the Na^+,K^+-ATPase activity have been described, most of which, including mastoparan, exert inhibitory action. Unexpectedly, 4 μM galparan activates Na^+,K^+-ATPase by 40%, while the effect of galanin and its fragments is negligible. The higher concentrations inhibit the enzyme as mastoparan does.

Transportan is a cell-penetrating peptide as judged by indirect immunofluorescence using K13-N^{ϵ}-biotinyl-transportan (*6*).The internalization of biotinyl-transportan is energy-independent and takes place efficiently at 37, 4, and 0 °C. Cellular uptake of transportan is probably not mediated by endocytosis since it cannot be blocked by treating the cells with phenylarsine oxide or hyperosmolar sucrose solution, and the uptake is nonsaturable. At 37 °C, the maximal intracellular concentration is reached in ∼20 min. The

† This study was supported by grants from the Swedish Natural Science Research Council and from EU program Contract MAS3-CT97-0156.

* To whom correspondence should be addressed.

‡ Department of Biochemistry and Biophysics.

§ Department of Neurochemistry and Neurotoxicology.

10.1021/bi0008985 CCC: $20.00
Published on Web 02/13/2001

internalized transportan is protected from trypsin. The cell-penetrating ability of transportan is not restricted by cell type, but seems to be a general feature of this peptide. In Bowes melanoma cells, transportan first localizes itself in the outer membrane and cytoplasmic membrane structures. This is followed by redistribution into the nuclear membrane and uptake into the nuclei where transportan concentrates in distinct substructures, probably the nucleoli. Despite many efforts, the mechanisms of cellular translocation of the peptide transporters are still largely unknown. The ability to associate with biomembranes seems to be a common denominator, and the activity of transportan does not seem to require a receptor since it has been seen in a variety of cell lines and is unchanged even at low temperatures when receptor-mediated endocytosis is blocked (*10*).

We have previously studied galanin and its association with and structure induction by biomembrane mimetic solvent systems (*11*). In the study presented here, we have extended this work to transportan. We have studied the properties of transportan when associated to SDS[1] micelles using CD and NMR spectroscopy, including the use of paramagnetic probes to localize the peptide relative to micelle geometry. The results have been compared to the previous studies on galanin and to new results on mastoparan alone.

The results show a significant interaction of transportan with the negatively charged SDS micelle, with concomitant induction of α-helical structure in the mastoparan part of the sequence. The peptide is mostly buried inside the hydrophobic interior of the micelle with some part exposed at the surface of the micelle. In terms of secondary structure, the properties of transportan resemble those of its constituent peptide parts. The location relative to the micelle surface should mimic the association of transportan with a phospholipid bilayer, and may suggest a partial explanation for the remarkable membrane translocating properties of the peptide.

MATERIALS AND METHODS

The mastoparan peptide was purchased from Sigma and the transportan peptide from Neosystem Laboratories (Strasbourg, France). Deuterated SDS was purchased from MSC Isotopes. The 5- and 12-doxyl-stearic acids were from Sigma, and the $MnCl_2$ was from Merck (Darmstadt, Germany). The methanol-d_4, used to dissolve the stearic acids, was purchased from Merck.

CD Spectroscopy. CD spectra were recorded on a JASCO J-720 spectropolarimeter equipped with a thermoelectrically controlled cell holder.

NMR Spectroscopy. NMR samples were prepared by dissolving the peptide powder at a concentration of 3 mM in 300 mM deuterated SDS solution in a mixture of H_2O and D_2O. Under the conditions that were used, SDS forms stable micelles at the level of 60 SDS molecules/micelle (*12*). The H_2O/D_2O ratio was 90/10. The pH was set to 3.1 by adding small amounts of HCl. The sample volume was 600 μL in a 5 mm sample tube.

The ^1H NMR spectra were collected using a Varian spectrometer (Varian Unity-600) with a 600 MHz proton frequency in the phase sensitive mode. A triple-resonance probe was used. The spectral width was 8000 Hz. The chemical shifts were referenced to TSPA. Spectra were processed using the vnmr program on a Sun sparc5 workstation. All spectra were collected at 45 °C.

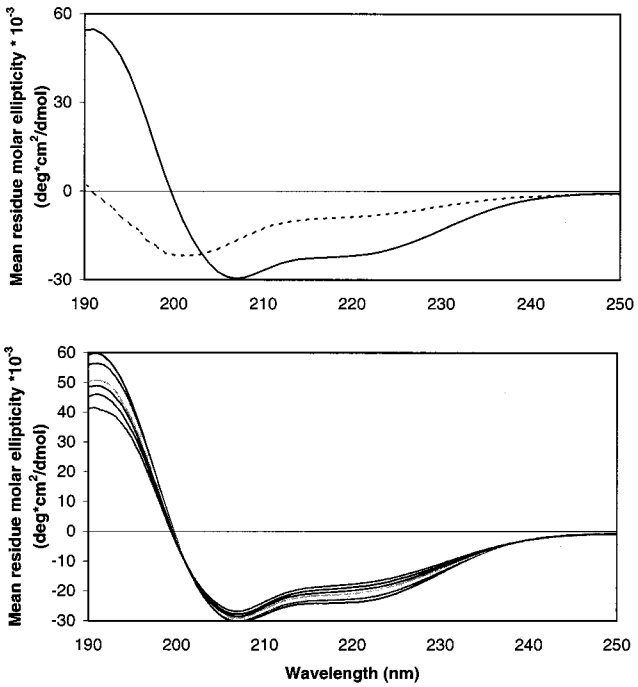

FIGURE 1: (Top) CD spectra of 40 μM transportan at 28 °C in water (- - -) and in a water/SDS solution (—) with 300 mM SDS. (Bottom) CD spectra of 40 μM transportan in 300 mM SDS at various temperatures between 5 and 65 °C.

One-dimensional ^1H spectra were recorded, achieving water suppression by presaturation, with 64 transients and 32K data points. Before Fourier transformation, the FID was zero-filled with 32K points. Two-dimensional NOESY (*13*) spectra were recorded with a mixing time, t_m, of 300 ms. The spectra were collected with 256 × 2048 data points. The number of transients was 32. Before Fourier transformation, the data were zero-filled with 2048 points. TOCSY (*14*) spectra were recorded with mixing times, t_m, of 30 and 60 ms. The spectra were collected with 256 × 2048 data points. The number of transients was 16. Before Fourier transformation, the data were zero-filled with 2048 points.

Spin-Label Experiments. The NMR samples were prepared by dissolving transportan at a concentration of 3 mM in 300 mM deuterated SDS solution in a mixture of H_2O and D_2O. If an SDS micelle aggregation number of 60 is assumed (*12*), this corresponds to a micelle concentration of 5 mM. The H_2O/D_2O ratio was 90/10. The 5- and 12-doxyl-stearic acids were solubilized in methanol-d_4 and then added to the samples to obtain a concentration of 5 mM, corresponding to at least one spin-label per micelle. The pH was set to 3.1 in all experiments.

Mn^{2+} Experiments. The sample was prepared by dissolving transportan at a concentration of 2 mM in a 300 mM deuterated SDS solution in a mixture of H_2O and D_2O. The H_2O/D_2O ratio was 90/10. The $MnCl_2$ was dissolved in H_2O before it was added to the sample. Experiments were performed with different concentrations of $MnCl_2$, from 200 μM to 3 mM. The pH was set to 3.1.

[1] Abbreviations: CD, circular dichroism; SDS, sodium dodecyl sulfate; TSPA, 3-trimethylsilyl-d_4 propionic acid; NOESY, two-dimensional nuclear Overhauser effect NMR spectroscopy; TOCSY, two-dimensional total correlated NMR spectroscopy.

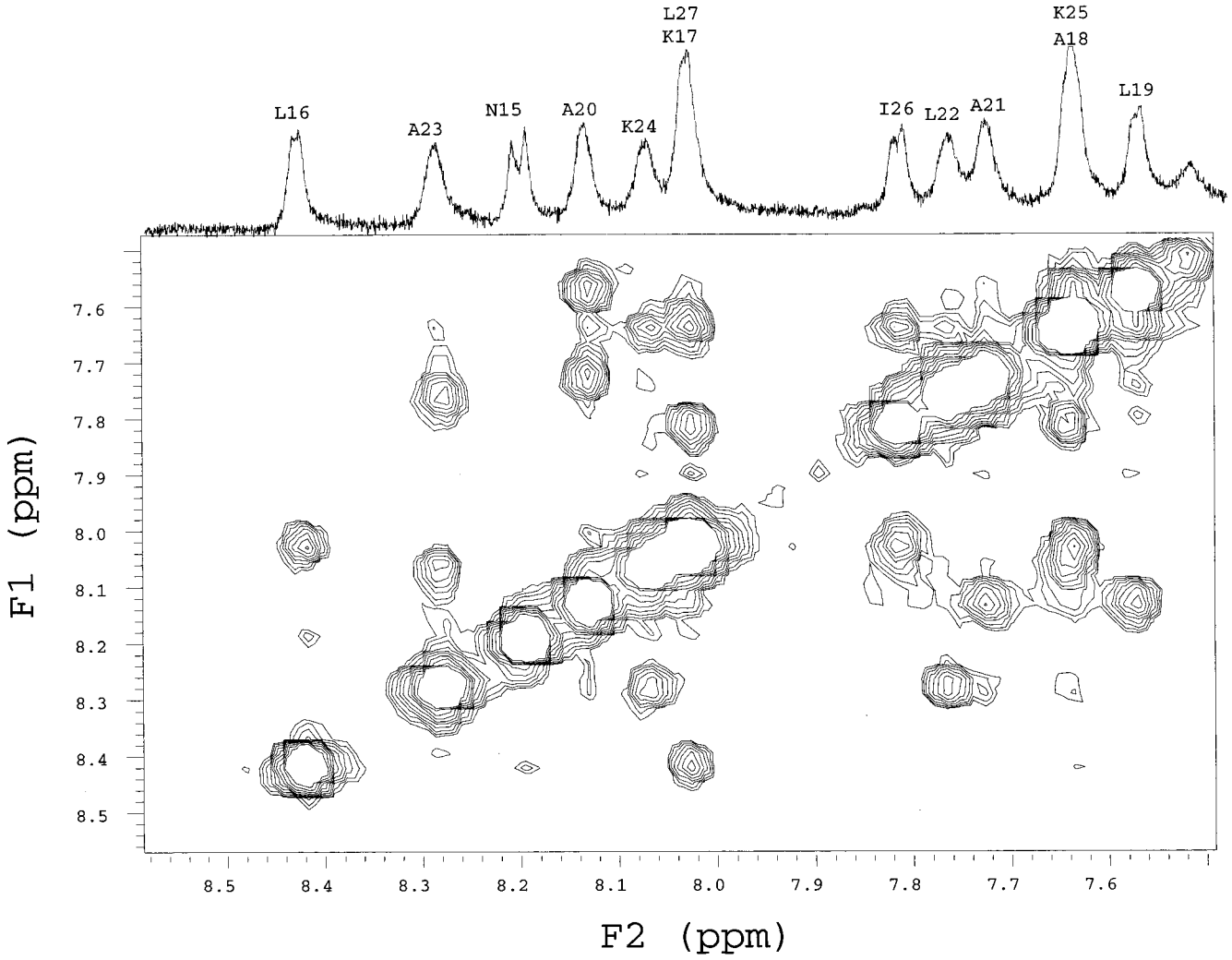

FIGURE 2: Partial 600 MHz two-dimensional NMR NOESY spectra (H^N-H^N region) of 1 mM mastoparan in 300 mM SDS at 45 °C and pH 3.1. At the top of the figure, the corresponding one-dimensional spectrum with assignments is shown.

RESULTS

CD Spectroscopy. CD spectra were recorded for transportan (Figure 1, top panel) and mastoparan (data not shown) in water and in 300 mM SDS in water. The conditions correspond to a micelle concentration of ~5 mM, well in excess of the peptide concentration of ~40 μM. From the mean residue molar ellipticities (dimensions, deg cm^2 dmol^{-1}) at 222 nm (−8000 for mastoparan in water, −27500 for mastoparan in SDS, −8000 for transportan in water, and −21400 for transportan in SDS), we estimated the following α-helical contributions of secondary structure in the peptides: 29% from mastoparan in water, 75% from mastoparan in SDS, 29% from transportan in water, and 60% from transportan in SDS. The estimations were based on the assumption that only random coil and α-helix secondary structures were present in the peptides, and on the standard values of the mean residue molar ellipticity at 222 nm, 4000 deg cm^2 dmol^{-1} for random coil and −38000 deg cm^2 dmol^{-1} for α-helix (*15*). Similar estimates for transportan were also obtained when the secondary structure content in the peptide was evaluated using a set of basis CD spectra. Figure 1 (bottom panel) shows the effect of a varying temperature on the transportan in SDS micelles. The structure induction is significant even at 65 °C, indicating that the peptide−micelle complex is also relatively stable at that temperature. There is essentially a two-state equilibrium, as evidenced by an isodichroic point at 202 nm.

Table 1: Assignment of Mastoparan ^{1}H NMR Resonances (300 mM SDS, pH 3.1, and 45 °C)[a]

residue[b]	HN	H^α	H^β	H(other)
Ile^{14} (1)	3.95	1.95	1.48	
Asn^{15} (2)	8.19	4.95	3.09, 2.84	
Leu^{16} (3)	8.42	4.05	1.87	1.59, 0.99, 0.86
Lys^{17} (4)	8.03	3.94		
Ala^{18} (5)	7.64	4.17	1.47	
Leu^{19} (6)	7.57	4.08	1.82	1.66
Ala^{20} (7)	8.12	3.95	1.50	
Ala^{21} (8)	7.74	4.05	1.52	
Leu^{22} (9)	7.78	4.10	1.83	
Ala^{23} (10)	8.28	3.90	1.45	
Lys^{24} (11)	8.07	3.88	1.93	
Lys^{25} (12)	7.66	4.06	2.03	
Ile^{26} (13)	7.81	3.95	1.87	0.93, 0.83
Leu^{27} (14)	8.02	4.21	1.77	1.57, 0.88

[a] Chemical shifts in parts per million relative to TSPA. [b] The residue numbering is taken from transportan. The original mastoparan numbering is in parentheses.

NMR Assignment. (1) Mastoparan. Figure 2 shows a partial ^{1}H NMR NOESY spectrum of mastoparan in 300 mM SDS at 45 °C used for assignment of the resonances. The

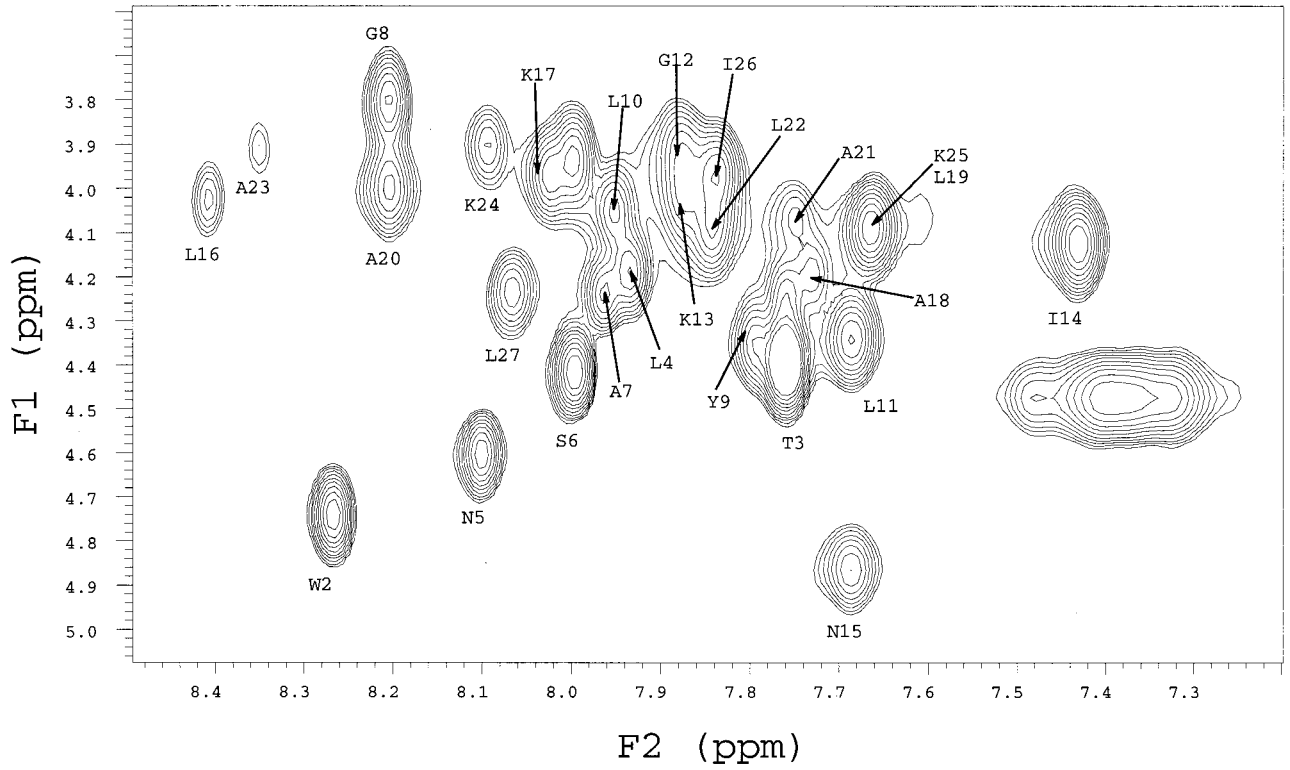

FIGURE 3: Partial 600 MHz two-dimensional NMR TOCSY spectrum ($H^{\alpha}-H^{N}$ region) of 2 mM transportan in 300 mM SDS at 45 °C and pH 3.1. The assignments of the cross-peaks are indicated.

Table 2: Assignment of Transportan ^{1}H NMR Resonances (300 mM SDS, pH 3.1, and 45 °C)[a]

residue		HN	H^{α}	H^{β}	H(other)
Gly[1]		3.88/3.79			
Trp[2]	8.27	4.74	3.24		
Thr[3]	7.76	4.40		1.15	
Leu[4]	7.94	4.19	1.65		
Asn[5]	8.10	4.61	2.82		
Ser[6]	8.00	4.44	3.95		
Ala[7]	7.96	4.24	1.45		
Gly[8]	8.21	4.00/3.79			
Tyr[9]	7.80	4.35	3.13		
Leu[10]		7.95	4.05	1.86/1.55	
Leu[11]		7.69	4.35	1.89/1.40	
Gly[12]		7.88	3.91		
Lys[13]		7.88	4.07		
Ile[14]	7.43	4.13	1.94	1.23/0.90	
Asn[15]		7.69	4.88	3.09/2.90	
Leu[16]		8.41	4.03	1.89	1.60
Lys[17]		8.02	3.99	1.93	1.47
Ala[18]		7.73	4.20	1.51	
Leu[19]		7.65	4.10	(1.79/1.66)	
Ala[20]		8.20	3.95	1.53	
Ala[21]		7.75	4.08	1.55	
Leu[22]		7.84	4.00(4.09)	1.86	0.95
Ala[23]		8.35	3.91	1.49	
Lys[24]		8.10	3.91	1.94	
Lys[25]		7.65	4.09	2.06	1.71
Ile[26]	7.84	3.97			
Leu[27]		8.07	4.25	1.82	1.59

[a] Chemical shifts in parts per million relative to TSPA.

assignment of mastoparan was straightforward using standard procedures. From the $H^{N}-H^{N}$ region in the NOESY spectra, we could assign the H^{N} protons. All H^{N} resonances were connected by (i,i+1) connectivities, in agreement with the observations of a high helical content from the CD studies. The TOCSY spectrum was then used to assign the rest of

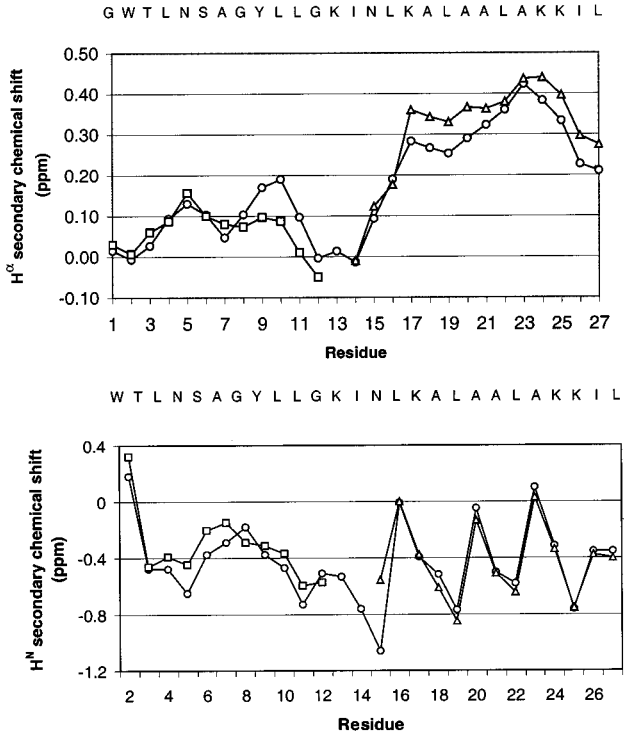

FIGURE 4: (Top) Secondary chemical shifts (H^{α}) for galanin (residues 1−12) (*18*), mastoparan, and transportan aligned along the peptide sequence which is indicated at the bottom of the diagrams. The secondary shifts are calculated as a mean value over three residues [shift(res^{i}−1) + shift(res^{i}) + shift(res^{i}+1)]/3. The secondary chemical shifts from transportan (○), galanin (residues 1−12) (□), and mastoparan (△) are shown. (Bottom) Secondary chemical shift (H^{N}) for galanin (residues 1−12) (*18*), mastoparan, and transportan aligned along the peptide sequence. The secondary chemical shifts from transportan (○), galanin (residues 1−12) (□), and mastoparan (△) are shown.

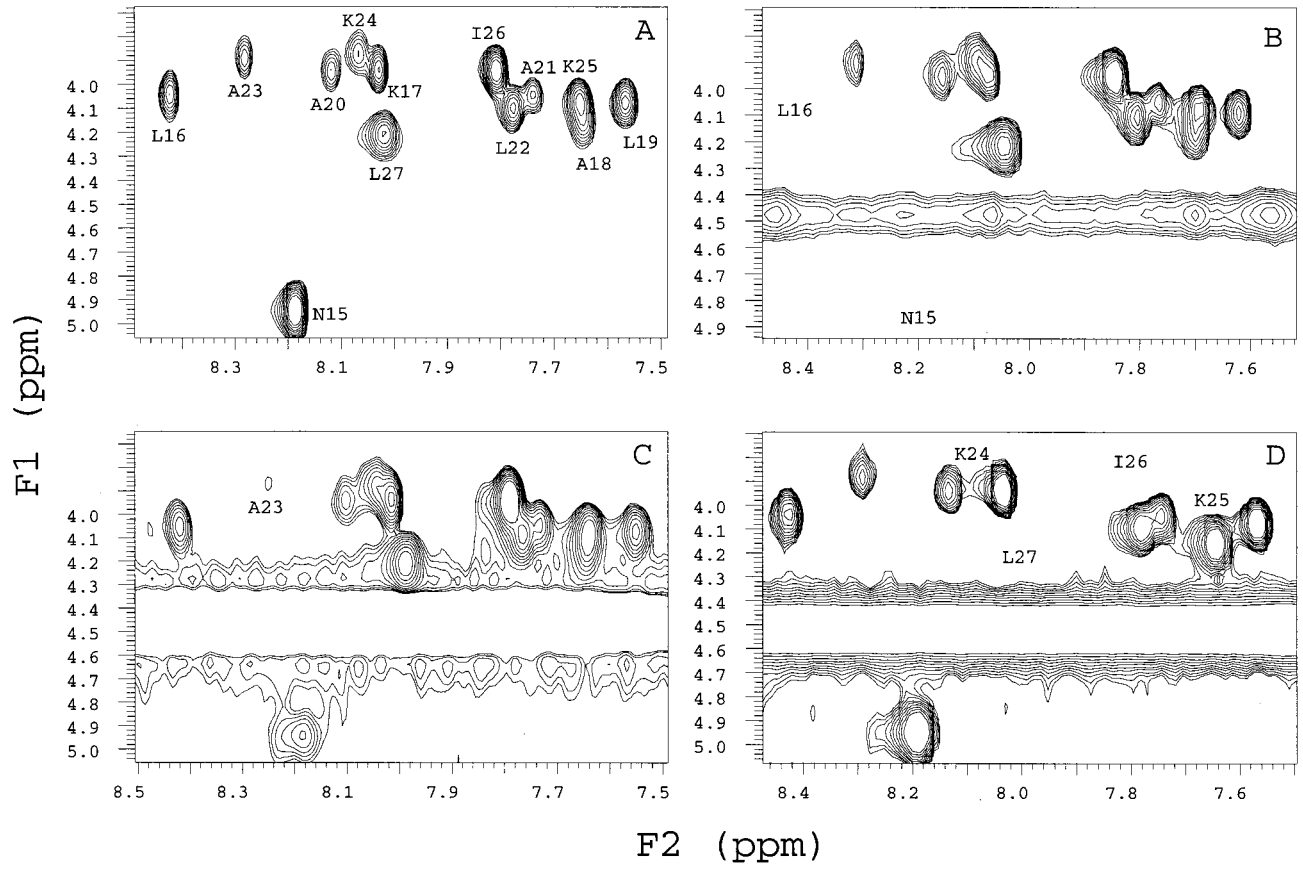

FIGURE 5: Partial 600 MHz TOCSY spectra ($H^{\alpha}-H^{N}$ region) of 1 mM mastoparan in 300 mM SDS at 45 °C and pH 3.1. (A) Spectrum for mastoparan without any paramagnetic agent present. (B) Spectrum with 5 mM 5-doxyl-stearic acid present. (C) Spectrum with 5 mM 12-doxyl-stearic acid present. (D) Spectrum with 1.5 mM $MnCl_2$ present. The indicated residues in panels B−D have lost their cross-peak intensities.

the spin systems. The starting point is the Asn^{15}, which has the characteristic β-proton resonances at 3.09 and 2.90 ppm. Table 1 summarizes the assignments.

(2) Transportan. Figure 3 shows a partial two-dimensional TOCSY spectrum of transportan in 300 mM SDS at 45 °C. Compared to that of mastoparan, the resolution of the NMR spectra of transportan was not as good, but assignments could be made using standard procedures (NOESY and TOCSY spectra). As shown in Figure 3, the $H^{\alpha}-H^{N}$ (so-called fingerprint) region has resolved cross-peaks for most of the residues. Table 2 shows the assignments. All cross-peaks in the $H^{\alpha}-H^{N}$ region were assigned (Figure 3).

Secondary Chemical Shifts. The secondary chemical shift ($\Delta\delta$) was calculated as the difference from the random coil chemical shift (δ_{RC}) as $\Delta\delta = \delta_{RC} - \delta_{measured}$. The random coil values are defined as the chemical shift for a residue, X, in the Gly-Gly-X-Ala peptide (*16*). To evaluate the secondary chemical shifts of the H^{α} proton resonances, the average of the secondary chemical shift ($\Delta\delta$) for the residue itself and the ones on either side was calculated. Secondary chemical shifts of the H^{α} resonances in peptides or proteins carry information about secondary structure: an upfield (positive) shift of 0.4 ppm is characteristic for an α-helix, whereas a downfield (negative) shift of 0.4 ppm is characteristic for a β-sheet (*17*).

Figure 4 (top panel) shows the H^{α} secondary chemical shifts of transportan and mastoparan in SDS micelles. For comparison, the corresponding data (residues 1−12) from the previous study on galanin in SDS (*18*) are also included. The results show that the secondary chemical shifts of transportan in SDS are very similar to those of its two component sequences, galanin (residues 1−12) and mastoparan. The high secondary shift values (0.3−0.4) of the mastoparan part both in mastoparan itself and in transportan show that there is almost complete α-helix secondary structure for this sequence in both samples. The N-terminal residues (1−12) apparently have very similar secondary structure in galanin and transportan. They were described as two relatively well-defined turns in SDS-bound galanin (type VII β-turn over residues 1−5 and 7−10) with some less structured residues surrounding them. A similar structure should prevail in this part of transportan.

Figure 4 (bottom panel) shows secondary chemical shifts of the amide (H^{N}) protons of mastoparan, transportan, and galanin (residues 1−12) (*17*). The reference data for a random coil were again taken from the Gly-Gly-X-Ala peptide (*16*). No averaging over residues was done in this case. Also, the H^{N} secondary chemical shifts are very similar in transportan and its two component peptides.

Paramagnetic Broadening Studies. To determine the position of mastoparan and transportan in the SDS micelle, we used the spin-labels 12-doxyl-stearic acid and 5-doxyl-stearic acid as well as Mn^{2+} ions ($MnCl_2$) to induce selective broadening of resonances from amino acids close to the paramagnetic probes. The doxyl group containing the spin-label free radicals is bound to carbon 12 or 5 of the stearic acid. Previous ^{13}C and ^{1}H NMR studies have shown that 12-doxyl-stearic acid particularly broadens resonances of

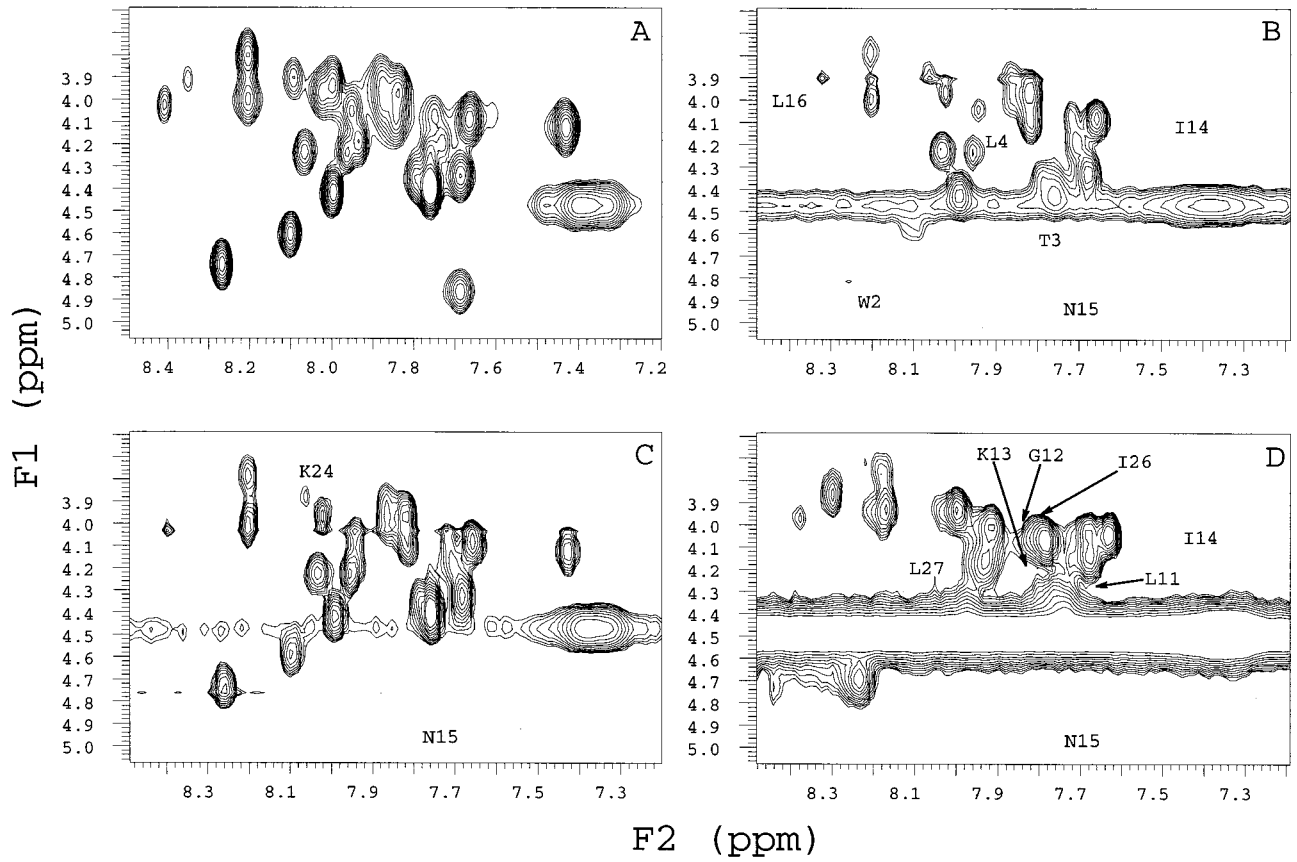

FIGURE 6: Partial 600 MHz TOCSY spectra ($H^{\alpha}-H^{N}$ region) of 2 mM transportan in 300 mM SDS at 45 °C and pH 3.1. (A) Spectrum for transportan without any paramagnetic agent present. (B) Spectrum with 5 mM 5-doxyl-stearic acid present. (C) Spectrum with 5 mM 12-doxyl-stearic acid present. (D) Spectrum with 1.5 mM $MnCl_2$ present. The indicated residues in panels B−D have lost their cross-peak intensities.

SDS carbons 10−12 and the corresponding protons close to the center of the micelle, whereas 5-doxyl-stearic acid broadens the resonances of SDS carbons 1−3 and the corresponding protons close to the micelle surface (*19*−*21*). At low concentrations, Mn^{2+} particularly affects resonances of water and the surface of an SDS micelle (*21*). The paramagnetic broadening effects of the agents on the peptide resonances were studied by comparing one-dimensional ^1H as well as two-dimensional TOCSY spectra in the presence and absence of the paramagnetic agents. The spin-label concentrations corresponded to one to four spin-labels per micelle, titrated into the NMR samples, with an assumed micelle concentration of 5 mM (60 SDS molecules per micelle). The Mn^{2+} was titrated into the NMR samples at concentrations from 0.2 to 3.0 mM.

Here we first show the results observed in the $H^{\alpha}-H^{N}$ region of TOCSY spectra after adding one spin-label per SDS micelle or 1.5 mM Mn^{2+} with mastoparan (Figure 5) and transportan (Figure 6). We observed that some cross-peaks were only marginally and uniformly affected by the addition of the paramagnetic probes, whereas other cross-peaks were broadened to the extent that they virtually disappeared from the two-dimensional spectra. The selective broadening was also confirmed in the $\alpha-\beta$ cross-peak region. To quantitatively interpret the results from the paramagnetic broadening experiments, we measured the maximum amplitude of each slice through a TOCSY $H^{\alpha}-H^{N}$ cross-peak, first without any paramagnetic agent and then compared to the amplitude from the corresponding cross-peak after adding the spin-label or Mn^{2+}. We normalized the amplitudes of the spectra with added paramagnetic agent to the least affected cross-peak and then calculated how much more the cross-peaks from other residues were affected. The results are shown in Figure 7a for mastoparan and Figure 7b for transportan. For transportan, we show the successive effects of adding two different concentrations of paramagnetic probes. In the TOCSY spectra (Figures 5 and 6), we have indicated disappearing cross-peaks which have lost more than 25% of the amplitude relative to those which are the least affected by the broadening agent (one spin-label per SDS micelle or 1.5 mM Mn^{2+}). These cross-peaks correspond approximately to those which are visually lost in the TOCSY spectra at the applied level of amplification.

(1) Mastoparan. Figures 5 and 7a show the effects of the paramagnetic broadening agents on the TOCSY $H^{\alpha}-H^{N}$ cross-peaks of mastoparan in SDS micelles. The data show some scatter, partly due to spectral overlap, but there is for the most part a clear pattern of neighboring residues behaving similarly with gradual changes along the sequence. To simplify the description, we will use the term "selective broadening" when 50−75% of the resonance amplitude was lost and "complete loss" when more than 75% was lost compared to the least affected resonance (with one spin-label per micelle or 0.5 mM Mn^{2+}). The addition of the 5-doxyl spin-label to the sample led to complete loss of cross-peaks from residues 15 and 16 (transportan numbering, here corresponding to the mastoparan peptide N-terminus) and selective broadening of resonances of residues 17, 18, and

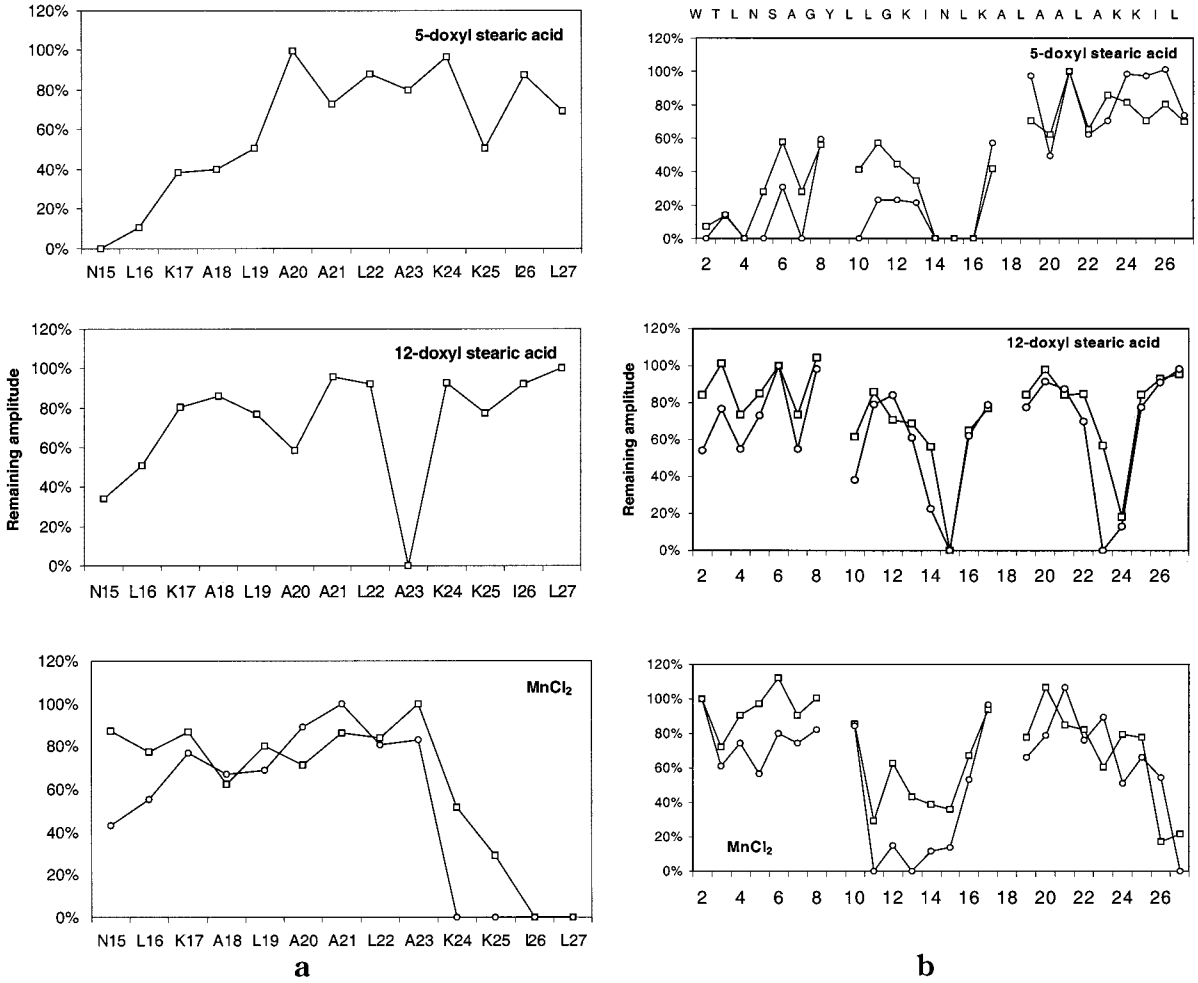

FIGURE 7: (a, left) Remaining amplitudes of $H^{\alpha}-H^{N}$ TOCSY cross-peaks of mastoparan in 300 mM SDS (Figure 5) after addition of paramagnetic probes. The top panel shows the remaining amplitude when 5-doxyl-stearic acid (one spin-label per micelle) is added. The middle panel shows the remaining amplitude when 12-doxyl-stearic acid (one spin-label per micelle) is added. The bottom panel shows the remaining amplitude when $MnCl_2$ [0.5 (□) and 1.5 mM (○)] is added. (b, right) Remaining amplitudes of $H^{\alpha}-H^{N}$ TOCSY cross-peaks of transportan in 300 mM SDS (Figure 6) after addition of paramagnetic probes. The top panel shows the remaining amplitude when 5-doxyl-stearic acid [one spin-label per micelle (□) and four spin-labels per micelle (○)] is added. The middle panel shows the remaining amplitude when 12-doxyl-stearic acid [one spin-label per micelle (□) and four spin-labels per micelle (○)] is added. The bottom panel shows the remaining amplitudes when $MnCl_2$ [0.5 (□) and 1.5 mM (○)] is added.

25. With the 12-doxyl spin-label, the cross-peak of residue Ala^{23} was completely lost and resonances of residues 15 and 16 were selectively broadened. With Mn^{2+}, cross-peaks from residues 24 and 25 were selectively broadened, with complete loss of the most C-terminal residues, 26 and 27.

(2) Transportan. Figures 6 and 7b show the effects of the paramagnetic broadening agents on the TOCSY $H^{\alpha}-H^{N}$ cross-peaks of transportan in SDS micelles. The 5-doxyl spin-label (one per micelle) gave rise to complete loss of cross-peaks from residues 2−4 and 14−16, and selective broadening of cross-peaks from residues 5, 7, 10, 12, 13, and 17. The 12-doxyl spin-label (one per micelle) caused complete loss of residues 15 and 24. Mn^{2+} ions (0.5 mM) selectively broadened cross-peaks from residues 11 and 13−15 and caused complete loss of cross-peaks from residues 26 and 27. Due to severe spectral overlap (Figure 3), the effects on cross-peaks of residues 9 and 18 could not be evaluated in transportan.

DISCUSSION

The CD experiments show that SDS induces a helical structure in both mastoparan and transportan. In mastoparan the helical content is 75%, and in transportan it can be calculated to be ∼55−65%, depending on temperature. The series of temperature-dependent spectra shows a clear isodichroic point (Figure 1, bottom panel), indicating a two-state equilibrium between random coil and α-helical secondary structure. The results show that the content of random coil increases with increasing temperature and that the helical content decreases.

The NMR assignments of both peptides were straightforward. The secondary chemical shifts (Figure 4) show that transportan secondary structure closely resembles its two separate parts, galanin (residues 1−12) and mastoparan. For the mastoparan α-helix, it is interesting to compare the present results in SDS with those reported for the same peptide in an isotropic solution of phospholipid bicelles (*22*). The secondary chemical shifts of the peptide amide proton resonances are quite similar in the two cases as shown in Figure 8. The periodic variation of the secondary chemical shifts in the bicelle solvent was suggested to originate from an asymmetric environment of the helix, with residues Leu^{16}, Ala^{20}, and Ala^{23} forming a helix face buried in the hydrophobic interior of the phospholipid bicelle environment (*22*).

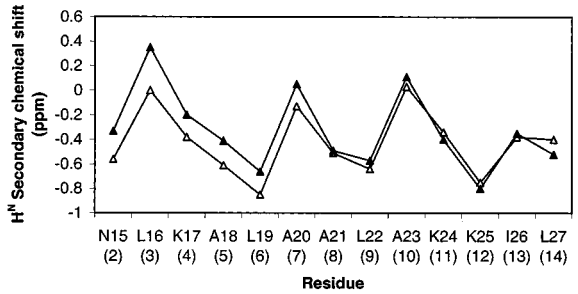

FIGURE 8: Secondary chemical shifts of amide protons for mastoparan in SDS micelles (△, present study) and in phospholipid bicelles (▲, from ref *22*). The residue numbering is taken from the transportan sequence. The original mastoparan numbering is shown in parentheses.

Our results are in agreement with this suggestion also for an SDS micelle environment, since we observe that particularly residues Ala^{20} and Ala^{23} are affected by the 12-doxyl-stearic acid probe (Figure 7a). This observed very close similarity between secondary structures induced in a detergent SDS micelle and a phospholipid bicelle is important, since it shows that in this respect the two solvent systems are rather equivalent.

The spin-label broadening results, when taken together with the Mn^{2+} results, give information about the location of the two peptides relative to the micelle geometry. When only the micelles and the paramagnetic agent are present, the broadening of resonances is rather selective and clear-cut (*21*). However, our results on the peptide/micelle system show that in some cases the same residue is strongly affected by more than one paramagnetic probe, suggesting that the specificity of the probes may be lower in this case. This must be related to the fact that the micelle is a very flexible system with the fatty chains moving freely and that the flexibility may even be increased when a peptide is added to the system (*21*). The dimensions of the peptide are also comparable with those of the SDS micelle. There is, however, nothing in our data to suggest that the overall geometry or properties of the micelle should be seriously changed by the presence of the peptide. It should also be pointed out that the overall Mn^{2+} concentration is low and below concentrations where one would expect to see effects on micelle size and structure.

Some conclusions about the location of the peptides can be drawn, by considering the quantitative evaluations in Figure 7. We first consider mastoparan. Figure 7a suggests three different segments which interact in different ways with the paramagnetic agents. N-Terminal residues 15−19, which interact most strongly with the 5-doxyl spin-label, should be close to but below the micelle surface. The central segment is buried inside the micelle since the 12-doxyl spin-label causes complete loss of the cross-peak of Ala^{23}. The C-terminus should be outside or at the surface, as indicated by the Mn^{2+} results on cross-peaks from residues 25−27.

We then consider transportan and compare its parts with the corresponding C-terminal mastoparan part (residues 14−27) and the N-terminal galanin part (residues 1−12). The mastoparan segment essentially follows the same pattern as mastoparan itself described above. The overall similarity suggests a similar positioning relative to the micelle as was described above for mastoparan. For the galanin part, we compare with the earlier reported experiments with galanin in SDS micelles (*18*). The earlier results with the same spin-labeled stearic acids showed that the 12-doxyl spin-label did not significantly broaden any cross-peak in the corresponding TOCSY region, similar to what was observed here for residues 1−12 of transportan. The 5-doxyl spin-label gave significant broadening of all residues in the region of residues 1−12 of galanin, except residues 6−9. For transportan, we note that the whole galanin region (residues 1−12) is to a varying degree affected by the 5-doxyl spin-label, with residues 6, 8, and 11 the least broadened, again a similar pattern as seen with the earlier galanin results. The overall similarity suggests that residues 1−12 of both galanin and transportan are positioned similarly in an SDS micelle, close to the micelle surface. In the present case, we also have the additional evidence from the Mn^{2+} results, which show that residues 11 and 12 together with Lys^{13} and mastoparan residues 14−16 form a central segment, affected by both

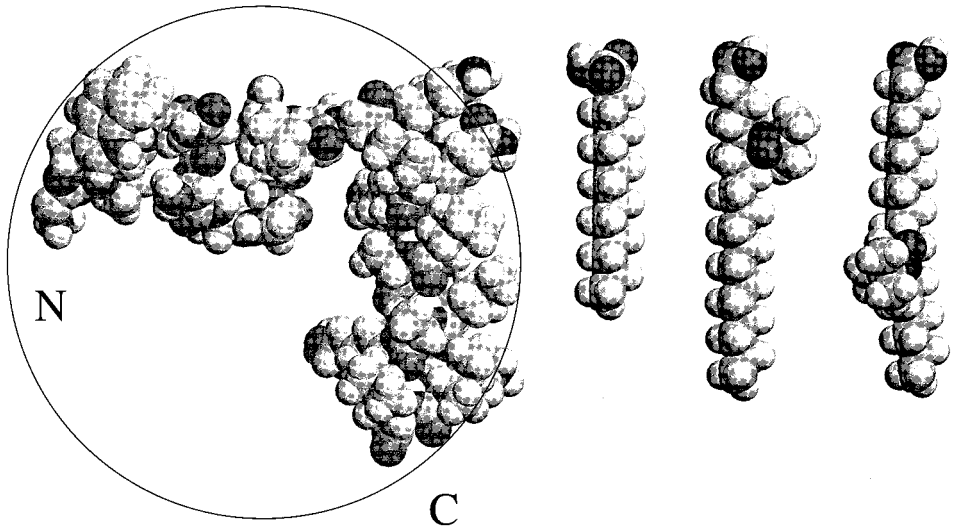

FIGURE 9: Schematic representation of transportan placed with a contour of an SDS micelle with a 35 Å diameter according to the paramagnetic probe results as described in the text. The N- and C-termini of transportan are indicated. The secondary structure of transportan is constructed from the ^1H NMR-determined structure of galanin (*18*) for residues 1−12, connected to Lys^{13} in an extended conformation and mastoparan residues 14−27 modeled as an α-helix with Leu^{27} in an extended conformation. For size comparison, the figure also shows, from left to right, SDS, 5-doxyl-stearic acid, and 12-doxyl-stearic acid.

the 5-doxyl spin-label and Mn^{2+}. Curiously, residue Asn^{15} is also strongly affected by the 12-doxyl spin-label. We have no ready explanation for this observation, except possibly unusual dynamic effects or a static disorder, particularly involving this residue. The ambiguity shows that it is important to use more than one paramagnetic probe in these systems, in order not to overestimate the precision in positioning that can be obtained from the results.

The overall conclusion from this study is that the secondary structures and positioning of the chimeric transportan peptide in an SDS micelle follow rather closely what is known about the two constituent segments. The strongly hydrophobic C-terminal mastoparan part seems to have the most profound contacts in the interior of the micelle, except for the outermost C-terminal residues, which may even be outside the micelle. The N-terminal galanin part prefers location close to but mostly below the surface. The connecting central segment of transportan is at or outside the surface.

Figure 9 is a graphical representation of the positioning of transportan relative to a schematic SDS micelle. Transportan was built from the calculated residues 1−12 structure of galanin in an SDS micelle (18), with an added K13 in an extended conformation, followed by residues 14−26 built in an ideal α-helical form and an extended L27. For size comparison, an SDS molecule and 5- and 12-doxyl-stearic acid molecules are also shown in the figure. The approximate diameter of an SDS micelle with an assumed spherical shape is ∼35−40 Å (*12*, *23*), also indicated in the figure. For mastoparan, the size of the micelle is large enough to harbor the helix inside, extending from below the surface on the N-terminal side to reach the surface on the C-terminal side. For transportan, we have introduced a bend at residue 13 to be able to fit the molecule inside the assumed SDS contour with only the central part and the C-terminal part outside.

The cartoon shown in Figure 9 raises the question of how a peptide structure in an SDS micelle may compare with the structure in a real biomembrane. The similarities in the amphiphilic nature of the constituents may be opposed by the differences in size between the detergent micelle and membrane. As was pointed out in ref *24*, the fact that the detergent micelle has dimensions comparable with a peptide gives a possibility that a larger regular secondary structure element, which could be formed in a membrane, may be broken in a micelle to gain free energy by exposing certain parts of it to the aqueous environment. On the other hand, a delicate energetic balance regarding the positioning relative to the micelle−membrane interior and surface for a peptide with charged as well as hydrophobic segments may be a critical factor for the mechanism that makes a peptide like transportan cross and carry cargo across hydrophobic membranes. A determination of the positioning of the various peptide segments in an extreme environment like an SDS micelle may therefore be relevant for understanding the transport mechanism.

ACKNOWLEDGMENT

We thank the NMR centre in Gothenburg, Sweden, for access to the NMR equipment. The expert technical assistance of T. Astlind and C. Damberg is gratefully acknowledged.

REFERENCES

1. Derossi, D., Joliot, A. H., Chassaing, G., and Prochiantz, A. (1994) *J. Biol. Chem. 269*, 10444−10450.
2. Derossi, D., Chassaing, G., and Prochiantz, A. (1998) *Trends Cell Biol. 8*, 84−87.
3. Elliott, G., and O'Hare, P. (1997) *Cell 88*, 223−233.
4. Liu, X., Timmons, S., Lin, Y., and Hawiger, J. (1996) *Proc. Natl. Acad. Sci. U.S.A. 93*, 11819−11824.
5. Zhang, L., Torgerson, T. R., Liu, X., Timmons, S., Colosia, A. D., Hawiger, J., and Tam, J. P. (1998) *Proc. Natl. Acad. Sci. U.S.A. 95*, 9184−9189.
6. Pooga, M., Hällbrink, M., Zorko, M., and Langel, Ü. (1998) *FASEB J. 12*, 67−77.
7. Lindgren, M., Hällbrink, M., Prochiantz, A., and Langel, Ü. (2000) *Trends Pharmacol. Sci. 21*, 99−103.
8. Consolo, S., Baldi, G., Nannini, L., Uboldi, M., Pooga, M., Langel, Ü., and Bartfai, T. (1997) *Brain Res. 756* (*1*−*2*), 174.
9. Östenson, C.-G., Zaitsev, S., Berggren, P. O., Efendic, S., Langel, Ü., and Bartfai, T. (1997) *Endocrinology 138* (8), 3308.
10. Mukherjee, S., Ghosh, R. N., and Maxfield, F. R. (1997) *Physiol. Rev. 77*, 760−790.
11. Öhman, A., Lycksell, P.-O., Andell, S., Langel, Ü., Bartfai, T., and Gräslund, A. (1995) *Biochim. Biophys. Acta 1236*, 259−265.
12. Israelachvili, J. (1991) *Intermolecular and surface forces*, p 372, Academic Press, San Diego.
13. Jeener, J., Meier, B., Bachman, P., and Ernst, R. R. (1979) *J. Chem. Phys. 71*, 4546−4563.
14. Braunschweiler, L., and Ernst, R. R. (1983) *J. Magn. Reson. 53*, 521−528.
15. Creighton, T. E. (1984) *Proteins*, p 181, Freeman, New York.
16. Wüthrich, K. (1986) *NMR of proteins and nucleic acids*, p 17, Wiley, New York.
17. Wishart, D. S., Sykes, B. D., and Richards, F. M. (1991) *J. Mol. Biol. 222*, 311−333.
18. Öhman, A., Lycksell, P.-O., Langel, Ü., Bartfai, T., and Gräslund, A. (1998) *Biochemistry 37*, 9169−9178.
19. Jarvet, J., Zdunek, J., Damberg, P., and Gräslund, A. (1997) *Biochemistry 36*, 8153−8163.
20. Papavoine, C., Konings, R., Hilbers, C., and van de Ven, F. (1994) *Biochemistry 33*, 12990−12997.
21. Damberg, P., Jarvet, J., and Gräslund, A. (2001) *Methods Enzymol.* (in press).
22. Vold, R. R., Prosser, R. S., and Deese, A. J. (1997) *J. Biomol. NMR 9*, 329−335.
23. Törnblom, M., Henriksson, U., and Ginley, M. (1994) *J. Phys. Chem. 98*, 7041−7051.
24. Russ, W. P., and Engelman, D. M. (1999) *Proc. Natl. Acad. Sci. U.S.A. 96*, 863−868.

BI0008985